

*Short Communication*

# Perforated Active Carbon and Pre-Lithiated Graphite Electrodes for High Performance Hybrid Lithium-ion Capacitors

Yifei Ren, Jing Li\*, Jianqiang Guo

School of Materials Science and Engineering, Southwest University of Science and Technology, Mianyang, Sichuan 621010, China

\*E-mail: [879763801@qq.com](mailto:879763801@qq.com)

Received: 31 October 2019 / Accepted: 26 November 2019 / Published: 10 February 2020

---

Lithium-ion capacitors are kinds of advanced energy storage systems, which possess performance of lithium-ion battery and electrical double layer capacitor. In this work, we have developed a new method to realize the pre-lithiation of graphite anode and fabricated lithium-ion hybrid capacitors with two cathodes including capacitor cathode (activated carbon) and battery cathode ( $\text{LiCO}_2$ ). The electrochemical performances indicate that the open-circuit voltage of the hybrid lithium-ion capacitor is nearly 0 V before the pre-lithiation. Finally, the voltage that rising with the process of pre-lithiation is up to 3.8 V. Meanwhile, the voltage of graphite electrode decreases from 3 V to 0 V vs  $\text{Li/Li}^+$ . The electrochemical results indicate that the capacitance of the hybrid lithium-ion capacitor decreased less than 1% after 300 cycles.

---

**Keywords:** Lithium-ion hybrid capacitor; Pre-lithiation;  $\text{LiCO}_2$ ; Activated carbon; Graphite

## 1. INTRODUCTION

With the growing requirements of high performance energy storage systems, it is urgent for developing hybrid power sources [1, 2]. Lithium-ion capacitor is a type of hybrid energy storage device which could bridge the gap between the lithium-ion battery and electrical double layer capacitor [3, 4]. The hybrid lithium-ion capacitors could deliver high energy density and power density at the same time [5]. As lithium-ion capacitors plays a significant role in the field of power devices, enhancing its energy density and power density has been one of the hot topic for science and engineering societies all over the world [6-8]. During the past decades, great achievements have been obtained for the lithium-ion capacitors, including design various anode and cathode materials [9-11].

Amatucci first used  $\text{Li}_4\text{Ti}_5\text{O}_{12}$  anode and active carbon cathode to prepare lithium-ion capacitor

[12]. After that the composite electrodes based  $\text{Li}_4\text{Ti}_5\text{O}_{12}$  anodes were reported as the anode materials for the lithium-ion capacitors, such as LTO/CNF [13], LTO/Ni-C [14]. And these works demonstrated superior electrochemical performance as anode materials for hybrid lithium-ion capacitors [15]. However, there is one disadvantage for the LTO-based anode materials, which has high intercalation/deintercalation potential about 1.55 V [16]. This will limit the voltage window of the lithium-ion capacitor with 1.5-3.0 V. As a result, the narrow voltage window leads to low energy density. According to the energy calculation equation, energy density is proportional to the capacitance and square of voltage window [17, 18]. As a result, the energy density can be improved by enhancing the voltage window of the lithium-ion capacitor. Besides, the transmission ability of lithium-ions in the electrolytes has great influence on the electrochemical performance of the hybrid lithium-ion capacitors. Sivakkumar used pre-lithiated graphite anode and activated carbon cathode to prepare lithium-ion capacitor, showing excellent rate capability and cycle performance [19]. The high performance is ascribed to the pre-doping methodology. Therefore, it is great important to improve the transport of lithium-ions.

In this paper, we developed hybrid lithium-ion capacitor with graphite anode and perforated active carbon cathode. The pre-lithiation of the graphite anode is achieved by using a perforated  $\text{LiCO}_2$  electrode. Meanwhile, a lithium foil is placed near the anode to monitor the potential change. The as prepared hybrid lithium-ion capacitor includes following advantages, a) the wide voltage window is beneficial for the improvement of energy density, b) the perforated AC and  $\text{LiCO}_2$  electrodes with uniform holes could promote the transportation of lithium-ions. As a result, the as-prepared hybrid lithium-ion capacitors display superior discharge and charge performance with a voltage window between 2.2 V to 3.8 V. Besides, the hybrid lithium-ion capacitor shows superior cycling performance, rate capability, as well as energy and power density.

## 2. EXPERIMENTAL

### 2.1 Preparation of electrode sheets

Graphite anode slurry was prepared by mixing graphite, carbon black, carboxymethylcellulose (CMC) and styrene butadiene rubber (SBR) with a ratio of 90:5:2:3. Then, the slurry was uniformly coated on the Cu film and dried at 80°C for 24 h. Similarly, activated carbon cathode slurry is made up of active carbon, carbon black, CMC and SBR with a weight ratio of 85:10:2:3.  $\text{LiCO}_2$  cathode slurry was prepared by the same way but the ratio of  $\text{LiCO}_2$ , SP, PVDF (90:5:5). The active carbon and  $\text{LiCO}_2$  cathode slurry were uniformly coated on the Al foil and dried at 110°C for 24 h. The active carbon and  $\text{LiCO}_2$  electrode sheets were perforated so that substantial lithium-ions could be intercalated into the graphite electrode.

### 2.2 Preparation of lithium-ion pouch capacitor

The capacitor was prepared according the following steps: firstly, graphite anode, separator,

activated carbon cathode, separator, LiCO<sub>2</sub> cathode were stacked together, which was then inserted into an aluminum-plastic bag by following an drying process for 24 h under vacuum and heating. Then, enough electrolytes were injected into the pouch capacitor. Moreover, a lithium foil was placed near the graphite anode, separated by a separator. At last, the aluminum-plastic package was heat-healed.

### 2.3 Electrochemical test

First, the pre-lithiation process was conducted for graphite by using LiCO<sub>2</sub> electrode. After pre-lithiation, galvanostatic charge/discharge test was conducted in the voltage range of 2.2~3.8 V under battery tester (LAND-CT2001A). Cyclic voltammetry (CV) measurement and electrochemical impedance spectra (EIS) were carried out on the electrochemical workstation (CHI660E).

## 3. RESULTS AND DISCUSSION

The photo of graphite anode, active carbon and LiCO<sub>2</sub> cathode is shown in Figure 1a. It can be observed that the active carbon and LiCO<sub>2</sub> cathode are perforated. This unique perforated design is determined to promote the transport of lithium-ions, which is beneficial for the pre-lithiation of the graphite anode. Figure 1b shows the photo of the hybrid lithium-ion capacitor. Four electrodes could be observed in the lithium-ion capacitor. The LiCO<sub>2</sub> cathode electrode is used for providing lithium-ions to obtain pre-lithiated graphite. Then, the active carbon cathode and pre-lithiated graphite anode form hybrid lithium-ion capacitor. Besides, the inserted lithium electrode is used for monitoring the voltage change at the same time.

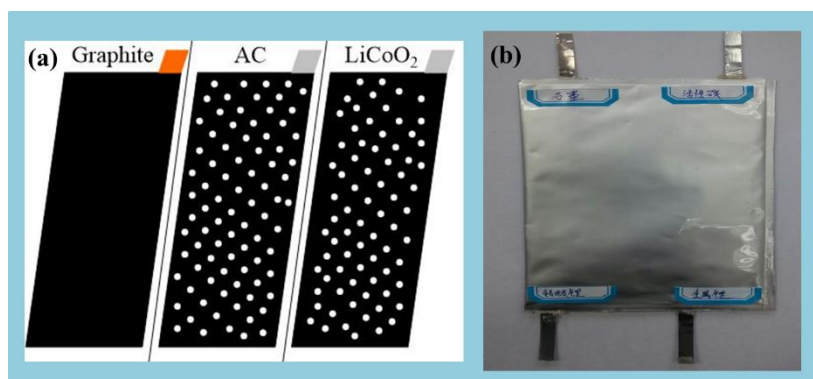


**Figure 1.** (a) Graphite, AC and LiCO<sub>2</sub> electrode films. (b) Photograph of the as-prepared hybrid lithium-ion capacitors.

The pre-lithiation is a critical step for LIC. To observe the voltage variation during the process of lithiation, voltage change of LiCO<sub>2</sub>/graphite was tested. As shown in Figure 2a, the voltage of LiCO<sub>2</sub>/graphite battery increases from 0 V to 4.2 V, indicating successful lithiation of the graphite electrode. Figure 2b shows the voltage change of AC/graphite electrode. It can be seen that the open-circuit of AC/graphite was nearly 0 V at the beginning. With the process of the lithiation of the graphite electrode, the voltage increases gradually. This demonstrates the electrochemical performance of hybrid lithium-ion capacitor. The curve of Figure 2c reveals the voltage of graphite electrode

decreases from nearly 3 V to 0 V [20].

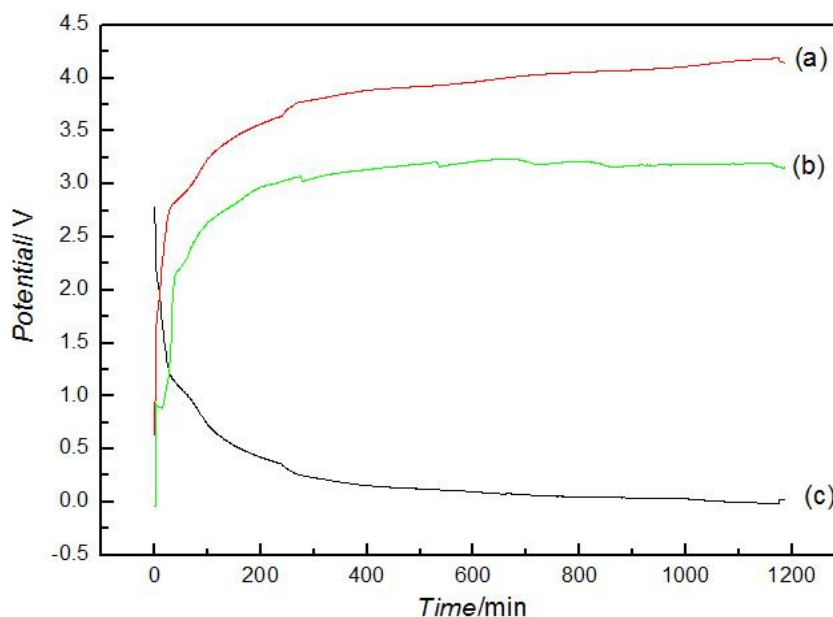


**Figure 2.** The potential variation curves (a) LiCO<sub>2</sub>/Graphite. (b) AC/Graphite. (c) Graphite/Li.

Figure 3 shows the voltage profile of the hybrid lithium-ion capacitor being charged and discharged from 2.2 to 3.8 V. In the voltage range from 2.2 to 3.8 V, the C/D curves display a nearly symmetrical triangle shape, demonstrating an ideal capacitive behavior. This is consistent with other reported works [21]. Furthermore, the voltage window of lithium-ion capacitor, which is about 3.8 V, is much higher than traditional supercapacitor (2.7 V). According to the following energy calculation equation [22], it can be concluded that the energy density will be highly improved.

$$E = \int V_c dQ = \int_{V_A}^{V_B} V_c d(CV) = \frac{1}{2} C(V_B^2 - V_A^2) = \frac{1}{2} CU^2$$

Here,  $E$  is the energy density,  $Q$  is the amount of charge,  $C$  is the specific capacity,  $U$  is the cell voltage.

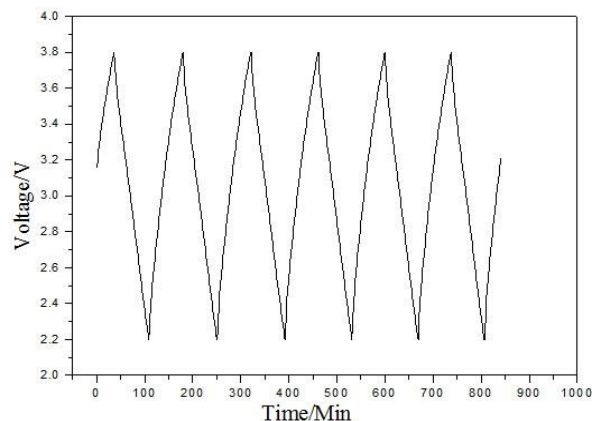


**Figure 3.** The constant charge/discharge curves of the as-prepared hybrid lithium-ion capacitors between 2.2 and 3.8 V.

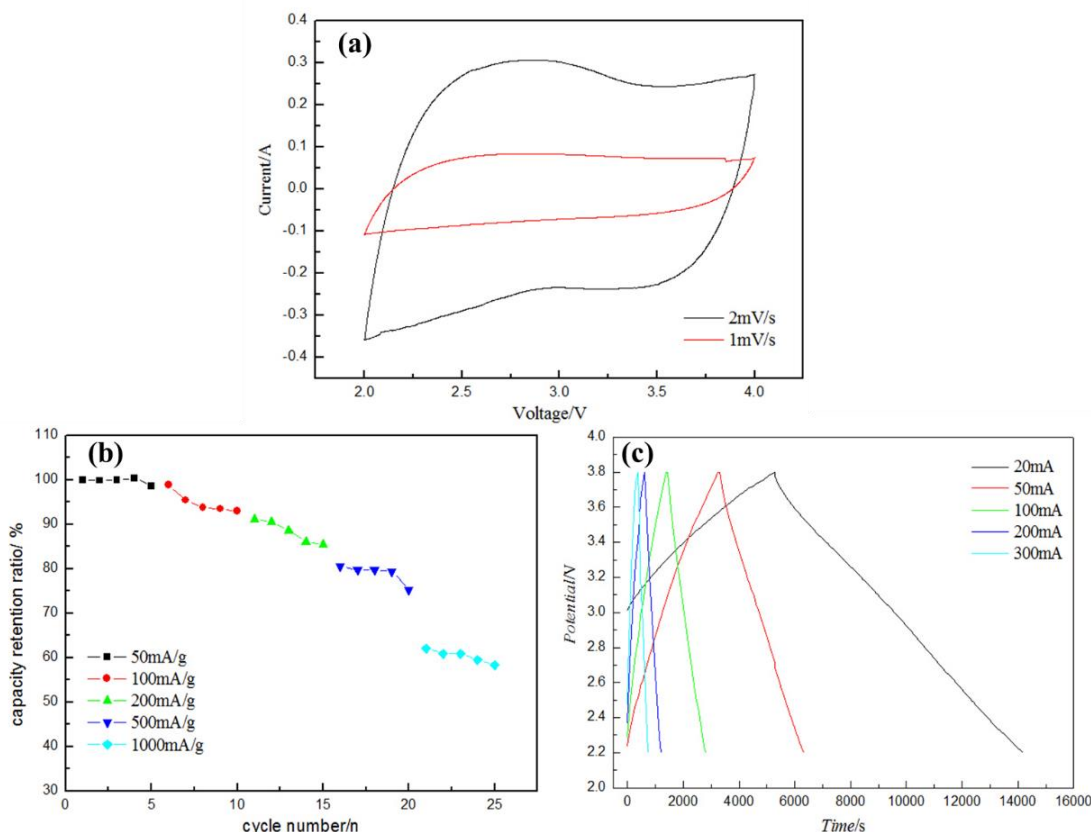


**Figure 4.** (a) Cyclic voltammogram curves of lithium-ion capacitor at different scan rate of  $1 \text{ mV}\cdot\text{s}^{-1}$  and  $2 \text{ mV}\cdot\text{s}^{-1}$ , respectively. (b) Rate capability of the hybrid lithium-ion capacitor at different current densities from  $50 \text{ mA g}^{-1}$  to  $1000 \text{ mA g}^{-1}$ . (c) The discharge and charge profiles of the hybrid lithium-ion capacitor.

Figure 4a shows the CV curves of lithium-ion capacitor at scan rate of  $1 \text{ mV s}^{-1}$  and  $2 \text{ mV s}^{-1}$ , respectively. In the voltage range from 2.2 to 3.8 V, the CV curves display a nearly rectangular shape, demonstrating an ideal capacitive behavior. Rate performance of hybrid lithium-ion capacitor was tested at various current densities from  $50 \text{ mA}\cdot\text{g}^{-1}$  to  $1000 \text{ mA}\cdot\text{g}^{-1}$ . As shown in Figure 4b, the as-prepared lithium-ion capacitors show high capacity retention at the current density of  $50 \text{ mA g}^{-1}$ . With the increase of the current density, the capacity fading can be observed. When the current densities are  $100 \text{ mA g}^{-1}$ ,  $200 \text{ mA g}^{-1}$  and  $500 \text{ mA g}^{-1}$ , the capacity retentions are 94%, 86% and 78%, respectively. Even at  $1000 \text{ mA g}^{-1}$ , the capacity retention could remain at 60%. Figure 4c shows the charge and discharge curves at various current densities. The discharge and charge curves exhibit linear and symmetric features. It can be concluded that the as-prepared hybrid lithium-ion capacitor shows perfect capacitor behavior. Besides, the gradient of curves is increasing with the improvement of current densities.

Figure 5a shows the cycling performance of lithium-ion capacitor at constant current during charge/discharge test. As shown in the figure, the hybrid lithium-ion capacitor displays an initial capacity of 75 F. After 300 cycles, the capacitance of hybrid lithium-ion capacitor decreases less than 1%. The reason of long-cycle performance is that the energy of hybrid lithium-ion capacitor is stored by electric double layers in cathode whose energy storage mechanism is different from lithium-ion battery [23]. The Nyquist plot of hybrid lithium-ion capacitor measured from 100 KHz to 10 mHz is

demonstrated in Figure 5b. The high frequency semicircle is ascribed to the charge-transfer resistance. Meanwhile, the inclined line at low frequency indicates pure capacitance characteristic. As expected, the result obtained from nyquist plot is consistent with the charge/discharge curve of the hybrid lithium-ion capacitor [24].

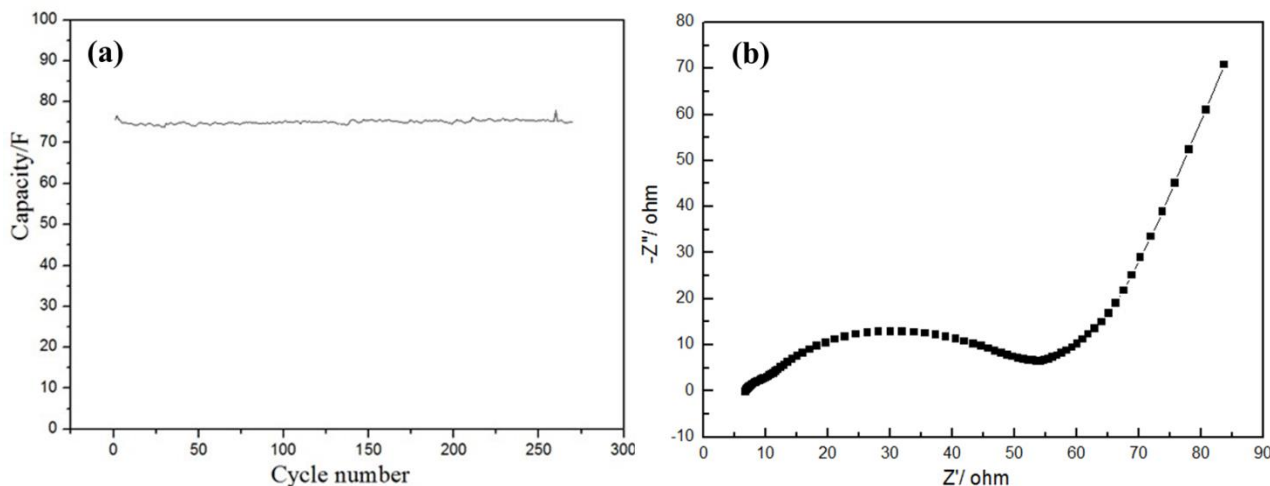


**Figure 5.** (a) The cycling performance of the hybrid lithium-ion capacitor at constant current (b) Nyquist plot of the hybrid lithium-ion capacitor.

The Ragone plots for the lithium-ion capacitor are demonstrated in Figure 6, obtained by calculating the energy and power density at various currents. The total mass of active materials is taken into consideration. With the increase of current from 20 to 300 mA, the energy densities are decreasing while power densities increasing. As a result, the lithium-ion capacitor exhibits a maximum power density of 74 W kg<sup>-1</sup> with an energy density of 25 Wh kg<sup>-1</sup> at the crossover point of 125 mA. Table 1 lists the electrochemical performance of various kinds of lithium-ion capacitors. It can be clearly observed that the as-prepared lithium-ion capacitor in our work shows higher capacity retention than other reported systems.

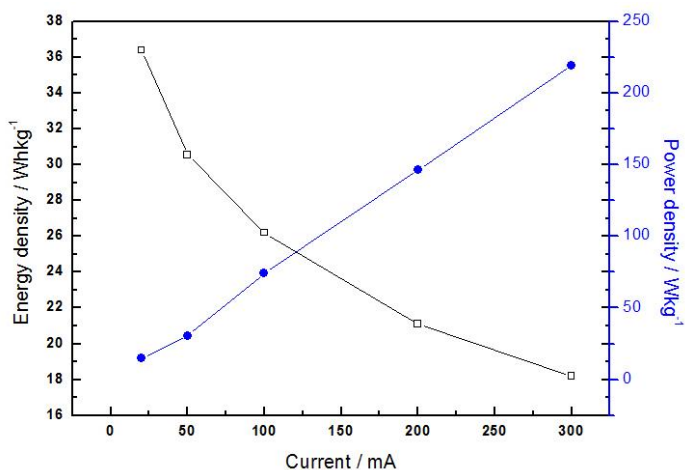


**Figure 6.** Ragone plots for the hybrid lithium-ion capacitor.

**Table 1.** The electrochemical performance of various kinds of lithium-ion capacitors.

| Li-ion Capacitor  | Capacity Retention (%) | Ref       |
|---|------------------------|-----------|
| Graphdiyne/AC   | 95                     | 25        |
| Graphite/AC Li <sub>4</sub> Ti <sub>5</sub> O <sub>12</sub> | 96                     | 26        |
| AC/HC   | 83                     | 27        |
| Nb <sub>2</sub> O <sub>5</sub> /C                           | 86                     | 28        |
| BG/TiO <sub>2</sub>   | 91                     | 29        |
| Graphite/AC/LiCO <sub>2</sub>                               | 99                     | This Work |

#### 4. CONCLUSION

In summary, we employed perforated LiCO<sub>2</sub> electrode as lithium source for the pre-lithiation of the graphite anode. Then, the hybrid lithium-ion capacitor consisted graphite anode and activated carbon cathode could deliver capacitor behavior. All the above process, including pre-lithiation and capacity release, could be achieved in one pouch device. It not only can be used lithium-ion battery, also lithium-ion capacitor. The electrochemical performance of the hybrid lithium-ion capacitor was tested when it plays a role of lithium-ion capacitor. The lithium-ion capacitor exhibits a maximum power density of 74 W kg<sup>-1</sup> with an energy density of 25 Wh kg<sup>-1</sup> at the crossover point of 125 mA. The capacity retention of the lithium-ion capacitor is as high as 99% after 300 cycles.

#### ACKNOWLEDGMENTS

This work was supported by Long Shan academic talent research supporting program of Southwest University of Science and Technology (Grant No. 17LZX507).

#### References

1. P. H. Smith, R. B. Sepe, K. G. Waterman and J. Myron, *J. Power Sources*, 327 (2016) 495.
2. J. Zhang, X. F. Liu, J. Wang, J. L. Shi and Z. Q. Shi, *Electrochim. Acta*, 187 (2016) 134.
3. Z. W. Yang, H. J. Guo, X. H. Li, Z. X. Wang, Z. L. Yan and Y. S. Wang, *J. Power Sources*, 329 (2016) 339.
4. C. X. Lu, X. Wang, X. Zhang, H. F. Peng, Y. G. Zhang, G. K. Wang, Z. K. Wang, G. L. Cao, N. Umirov and Z. Bakenov, *Ceram. Int.*, 43 (2017) 6554.
5. T. Xing, Y. H. Ouyang, L. P. Zheng, X. Y. Wang, H. Liu, M. F. Chen, R. Z. Yu, X. Y. Wang and C. Wu, *J. Energ. Chem.*, 42 (2020) 108.
6. C. Liu, Q. Q. Ren, S. W. Zhang, B. S. Yin, L. F. Que, L. Zhao, X. L. Sui, F. D. Yu, X. F. Li, D. M. Gu and Z. B. Wang, *Chem. Eng. J.*, 370 (2019) 1485.
7. M. Arnaiz, V. Nair, S. Mitra and J. Ajuria, *Electrochim. Acta*, 304 (2019) 437.
8. X. Li, Y. Tang, J. H. Song, M. S. Wang, Y. Huang, L. Liu and J. M. Zheng, *J. Alloy Compd.*, 790 (2019) 1157.
9. M. Hagen, J. Yan, W. J. Cao, X. J. Chen, A. Shellikeri, T. Du, J. A. Read, T. R. Jow and J. P. Zheng, *J. Power Sources*, 433 (2019) 126689.
10. H. N. Yang, C.K. Zhang, Q. H. Meng, B. Cao and G. Y. Tian, *J. Power Sources*, 431 (2019) 114.
11. C. Yang, J. L. Lan, C. F. Ding, F. Wang, S. H. Siyal, Y. H. Yu and X. P. Yang, *Electrochim. Acta*, 296 (2019) 790.

12. F. B. Amatucci, A. D. Pasquier and T. Zheng, *J. Electrochem. Soc.*, 148 (2001) A930.
13. L. Li, C. Jia, Z. Q. Shao, K. Chen, J. Q. Wang and F. J. Wang, *Chem. Eng. J.*, 370 (2019) 508.
14. M. X. Tran, A. Y. Kim and J. K. Lee, *App. Surf. Sci.*, 461 (2018) 161.
15. W. J. Na, A. S. Lee, J. H. Lee, S. M. Hong, E. Kim and C. M. Koo, *Solid State Ionics*, 309 (2017) 27.
16. C. Li, S. Cong, Z. N. Tian, Y. Z. Song, L. H. Yu, C. Lu, Y. L. Shao, J. Li, G. F. Zou, S. X. Dou, J. Y. Sun, Z. F. Liu, *Nano Energ.*, 60 (2019) 247.
17. J. Zhang, J. Wang, Z. Q. Shi and Z. W. Xu, *Chinese Chem. Lett.*, 29 (2018) 620.
18. K. Wang, N. Wang, J. J. He, Z. Yang, X. Y. Shen and C. S. Huang, *Electrochim. Acta*, 253 (2017) 506.
19. S. R. Sivakkumar and A. G. Pandolfo, *Electrochim. Acta*, 65 (2012) 280.
20. X. Z. Sun, X. Zhang, W. J. Liu, K. Wang, C. Li, Z. Li and Y. W. Ma, *Electrochim. Acta*, 235 (2017) 158.
21. C. Li, X. Zhang, K. Wang, X. Z. Sun and Y. W. Ma, *Carbon*, 140 (2018) 237.
22. F. M. Auxilia, J. Jang, K. H. Jang, H. Y. Song and M. H. Ham, *Chem. Eng. J.*, 362 (2019) 136.
23. X. Z. Sun, X. Zhang, H. T. Zhang, N. S. Xu, K. Wang and Y. W. Ma, *J. Power Sources*, 270 (2014) 318.
24. Q. Lu, B. Lu, M. F. Chen, X. Y. Wang, T. Xing, M. H. Liu and X. Y. Wang, *J. Power Sources*, 398 (2018) 128.
25. H. P. Du, H. Yang, C. S. Huang, J. J. He, H. B. Liu and Y. L. Li, *Nano Energ.*, 22 (2016) 615.
26. T. Rauhala, J. Leis, T. J. Kallio and K. Vuorilehto, *J. Power Sources*, 331 (2016) 156.
27. M. Arnaiz, V. Nair, S. Mitra and J. Ajuria, *Electrochim. Acta*, 304 (2019) 437.
28. H. X. Li, J. T. Chen, B. J. Yang, K. J. Wang, X. Zhang, T. Y. Zhang, L. Zhang, W. S. Liu and X. B. Yan, *Electrochim. Acta*, 299 (2019) 163.
29. J. P. Gao, G. J. Qiu, H. J. Li, M. J. Li, C. P. Li, L. R. Qian and B. H. Yang, *Electrochim. Acta*, 329 (2020) 135175.